Acta Biomed 2019; Vol. 90, Supplement 5: 68-76 DOI: 10.23750/abm.v90i5-S.8326

Review

Application of diffusion tensor imaging (DTI) and MR-tractography in the evaluation of peripheral nerve tumours: state of the art and review of the literature

Federico Bruno[1], Francesco Arrigoni[1], Silvia Mariani[1], Lucia Patriarca[1], Pierpaolo Palumbo[1], Raffaele Natella[2], Liheng Ma[3], Giuseppe Guglielmi[4], Renato J Galzio[5], Alessandra Splendiani[1], Ernesto Di Cesare[1], Carlo Masciocchi[1], Antonio Barile[1]

[1] Department of Biotechnology and Applied Clinical Sciences, University of L'Aquila, L'Aquila, Italy; [2] Department of Precision Medicine, University of Campania "L. Vanvitelli", Napoli; [3] Department of Radiology, GuangDong Pharmaceutical University, Guangzhou, Cina; [4] Department of Clinical and Experimental Medicine, Foggia University School of Medicine, Foggia, Italy; [5] Neurosurgery, "San Salvatore" Hospital, L'Aquila

Summary. Peripheral nerves can be affected by a variety of benign and malignant tumour and tumour-like lesions. Besides clinical evaluation and electrophysiologic studies, MRI is the imaging modality of choice for the assessment of these soft tissue tumours. Conventional MR sequences, however, can fail to assess the histologic features of the lesions. Moreover, the precise topographical relationship between the peripheral nerve and the tumor must be delineated preoperatively for complete tumour resection minimizing nerve damage. Using Diffusion tensor imaging (DTI) and tractography, it is possible to obtain functional information on tumour and nerve structures, allowing the assess anatomy, function and biological features. In this article, we review the technical aspects and clinical application of DTI for the evaluation of peripheral nerve tumours. (www.actabiomedica.it)

Key words: peripheral nerve tumours, schwannoma, neurofibroma, diffusion imaging, dti, tractography

Introduction

Peripheral nerve tumors (PNTs) are rare (less than 5% of tumors of the hand and upper extremities) and include benign lesions (mainly schwannomas and neurofibromas) and malignant lesions (malignant neurofibromas, also termed as malignant peripheral nerve sheaths tumors, MPNSTs) (1-3). PNTs are usually slow-growing masses, and about six people out of 1 million undergo surgery for these tumors each year, with a risk of developing a malignant PNST of about 0.001% in the general population (8-13% in patients with neurofibromatosis Type 1) (2).

Tumors may be intraneural involving 1 or multiple nerve fascicles, splaying apart them, or may be attached to a superficial fascicle and thereby displacing the remainder of the nerve (4, 5).

The diagnosis of PNTs is based primarily on the clinical examination, and instrumental evaluation using ultrasound and electrophysiologic studies are the first steps for diagnosing PNTs (6). MRI, due to its intrinsic excellent soft tissue contrast and the absence of ionizing radiations compared to CT (7), is a valuable diagnostic tool for the diagnosis and the guidance of interventional procedures in a wide range of organs and systems (8-19), and in peripheral nerve imaging as well (20-22). In particular, imaging plays a key role for the preoperative and postoperative evaluation (21, 23-30). However, two main limitations of standard MRI sequences are the low specificity for the discrimina-

tion of benign and malignant PNSTs (even when MRI findings such as nerve thickening, necrosis, infiltration, hemorrhage, inhomogeneous enhancement, pose for malignant tumor lesions) and the challenging delineation of the tumor and healthy nerve fascicles involvement (31, 32). Histological confirmation is often necessary to make a definitive diagnosis (33-36). Interventional radiology procedures are widely used for the treatment of most soft tissue lesions (37-48), but surgical removal is the definitive treatment for peripheral nerve tumours. As surgery for PNTSTs may result in a considerable neurological deficit, the primary goal is the preservation of unaffected nerve fibers. Currently, appropriate surgical planning is mainly based on intraoperative findings of electrophysiological monitoring and high-resolution ultrasound (49), even if the resolution is not sufficient to identify relations between tumor and individual nerve fascicles (50). Many advanced MRI sequences have been developed to provide additional anatomical and functional information to standard MR examination (12, 51, 52), and in this scenario, DTI application with tractography, already studied in chronic compressive neuropathies and traumatic nerve injuries, is being applied with increasing frequency to allow the diagnosis and the preoperative assessment of peripheral nerve tumors (53).

The purpose of this article is to review the technical aspects of this advanced MR imaging technique, with a particular focus on its clinical application in patients with peripheral nerve tumors.

Basic principles of DTI imaging

Diffusion tensor imaging (DTI) is an extension of diffusion-weighted imaging (DWI), a well-known technique that measures the magnitude of random displacement of water molecules and that is widely used for the diagnosis of different pathologic entities across a range of organ systems (54). Diffusion tensor imaging (DTI) evaluates the direction of the diffusion as well, differentiating isotropic tissues - in which water molecules show equal diffusion in all directions - and anisotropic tissues (such as neural tissue or other tissues displaying ordered and oriented fibers), in which diffusion is predominant in one direction (principal eigenvector) (55). The sequence involves the application of diffusion-sensitizing gradients in multiple directions, allowing diffusion to be displayed as vectors representing the characteristics of diffusion and anisotropy along the spatial axes. Fractional anisotropy (FA) is the overall measure of tissue anisotropy with values between 0 to 1 (from complete isotropic diffusion to completely directional diffusion) (56, 57).

Other parameters derived from DTI are: the mean diffusivity (MD), that is the average of three diagonal elements of the diffusion tensor, the axial diffusivity (AD), that is the direction of the largest eigenvector, and the radial diffusivity (RD), that is an average of the two smaller tensor eigenvalues (4, 58). Several evidences demonstrated the correlation of DTI parameters with electrophysiology and histology and their validity in characterizing nerve injury. In particular, lower FA values represent nerve injury (due to loss of directional diffusion), AD reflects axon integrity, and RD (and FA) correlates with myelin sheath integrity (59) (Fig. 1). Tractography exploits DTI data to generate 3D representations based on voxel fractional anisotropy values. Using color maps, fibers extending superior-inferiorly are colored blue; those extending left-right are colored red, and those extending anterior-superiorly are colored green. Other directions are represented by a combination of these colors (50) (Fig. 2).

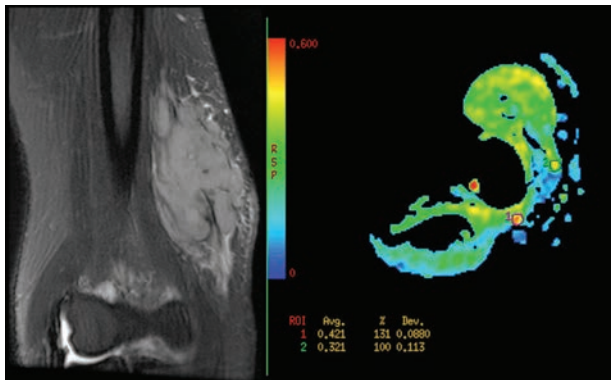

Figure 1. Coronal T2 fs sequence in a patient with a soft tissue mass involving the ulnar nerve . In the right picture, FA map of the DTI sequence with ROI positioning showing reduced FA values of the ulnar nerve at the level of the lesion, consistent with axonal damage

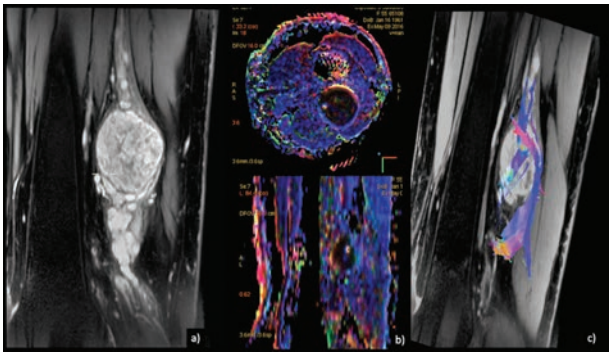

Figure 2. Sagittal contrast enhanced MR slice (a) showing a polylobate fusiform lesion between the biceps femuris and the semitendinosus muscles. FA colored maps in which diffusion vector directions are displayed in different colours (b). In c, tractographic 3D reconstruction

DTI imaging acquisition in peripheral nerve imaging: technical notes

Peripheral nerve DTI can be performed clinically without need of contrast medium administration (60-63), either with 1.5T and 3.0T scanners. Higher field strength, despite the higher SNR, exacerbates the effects of magnetic field inhomogeneities, so the use of localized shim regions is recommended (59). Experiences with peripheral nerve DTI at extremely high field strengths, such as 7.0T, are limited due to the need of specific transmit and receive coils, power deposition concerns, and susceptibility distortions in echo-planar imaging. Having MR imaging systems with a high slew rate is also important. High-channel surface phase-array *coils* can be used as close to the anatomy of interest for both upper and lower extremities. In our clinical practice, we use a multi-channel "flex" coil (small, medium, or large). Torso or spine coils can be used for the lumbosacral plexus (64, 65).

The most commonly DTI *sequence* is a single-shot, 2D EPI (SSEPI). This sequence allows obtaining high SNR with relatively short imaging and consequently few potential motion artifacts (6). Multishot sequences allow higher spatial resolution with higher SNR, with the drawback of more severe motion artifacts and increased scan time. EPI sequences can also be affected by other artifacts, such as chemical shift, ghost artifacts, T2-related blurring, and susceptibility artifacts due to magnetic field inhomogeneities. It is possible to minimize such artifacts using spectral fat suppression, shorter echo-train lengths, tighter echo spacing, higher bandwidth, shimming, and motion correction techniques. The number of acquisitions may be increased, but with consequent longer scanning time and possible motion artifacts (31).

Parallel imaging techniques can be used to reduce imaging time, but an acceleration factor of 2 is usually used, as higher acceleration factors can affect SNR and cause foldover artifacts.

The TR is in the order of 3000 to 4500 milliseconds, and it depends on the anatomic coverage. The TE ranges from 40 milliseconds to 80 milliseconds, depending on the b value and the gradient strength (66). The FOV is adjusted to the anatomy to be covered, typically 140 x 140 mm to 240 x 240 mm.

The *b value* is the main parameter of a diffusion-weighted sequence, representing the strength, duration, separation, and amplitude of the diffusion gradients (66-68). Several studies report the appropriate range of b values for peripheral nerve DTI, with values ranging from 400 to 1000s/mm. In our experience, a b-value of 600s/mm2 is sufficient to reliably track most peripheral nerves in the extremity and provides a good balance of diffusion weighting and SNR (69). Higher b-values increase the diffusion weighting but reduce the SNR. The images are also acquired with a b value of 0, before the application of diffusion gradients. Conversely, low b values can lead to erroneous tracking of low anisotropy structures (such as subcutaneous fat).

DTI of peripheral nerves requires at least six non-colinear *gradient directions*. A greater number of directions sampled increases the accuracy of diffusion measurements, but at the cost of increased imaging time. There is no universal agreement in the literature about the optimum number of gradient directions for the different peripheral nerves, with values ranging from a minimum of six directions at 1.5T to as many as 25 gradient directions at 3.0T (70).

Several stand-alone and vendors specific *dedicated software* can be used to evaluate DTI parameters (FA, ADC, MD) (56, 71). Tractographic images are created connecting adjacent voxels with similar anisotropy values. Measurements are made using regions of interest (ROI) positioning at specific sites along the nerve over the structure being investigated. The qual-

Table 1. Scanning parameters suggested for MR DTI sequence (ssEPI)

DTI PARAMETERS
▪ Spin-echo-single-shot EPI sequence
▪ Axial plane
▪ b-value: 0, 1000s/mm2
▪ 25 diffusion gradient orientations
▪ Slice 3 mm - no interslice gap
▪ TR: 8400ms
▪ TE: minumum
▪ NEX: 3
▪ FOV: 140x140 - 250x250mm
▪ Matrix: 96x96 - 256x256
▪ Shimming

ity of the tractography images partly depends on the thresholds that are applied for FA values and the turning angle of the eigenvectors between adjacent voxel, as optimal parameters vary depending on the geometry of the nerve studied (65). Usually, two thresholds are applied: minimum FA (typically >0.3) and turning angle of diffusion vectors (typically >278) to maintain optimal tracking of peripheral nerve bundles. Choosing the highest or lowest values can result in the tracking of adjacent anatomic structures (muscle or vessels) or the possible exclusion of nerve portions.

Acquisition parameters proposed from our experience are summarized in Table 1.

Clinical application of DTI in peripheral nerve tumours

In one of the first reports from Chabra et al. (58) on 29 patients with surgically proved peripheral nerve tumours, the FA of involved nerves was significantly lower than that of contralateral nerves (as a likely indirect sign of axonal degeneration and myelin loss) with excellent interobserver reliability. ADC values measured on DTI and DWI sequences in the same patients were comparable. DWI ADC was not able to differentiate benign and malignant lesions, while ADC on DTI resulted to be more useful for this discrimination; these findings may be explained by the higher number of directions in diffusion encoding and higher b-values used in their DTI technique (1000 s/mm2 versus 800 s/mm2). Additionally, among the benign lesions, ADC in 12-direction DTI was not statistically different from 20-direction DTI. On tractography, most benign lesions showed partial tract disruption or near-normal appearance except a degenerated schwannoma and a plexiform neurofibroma, in which there was complete tract disruption. They did not observe an isolated course deviation as a sign of BPNST as reported in a feasibility study by Vargas et al. (72-78), explaining these findings with the presence of axonal degeneration and/or myelin loss that result in local loss of fiber attenuation, even with intact anatomic fascicular architecture. Cases of MPNSTs showed partial and complete disruption of tracts, findings that were also confirmed surgically. The near-normal appearance of the tracts was also seen in lymphoma, CMT, and perineurioma; which are explainable by the permeative nature of lymphoma. 20% of the lesions could not be traced due to suboptimal SNR/ghosting artifacts. Higher ADC as an indicator of the benignity of lesions was also confirmed in other tumors, such as breast and prostate. They also suggested the use of ADC as a potential biomarker, due to its excellent interobserver reliability, to detect tumor response/necrosis during chemotherapy.

Also Schmidt et al. showed good preoperative nerve fascicle visualization using DTT scans in 83% of patients, with a good intraoperative correlation between DTT scans and surgical anatomy.

Cage et al. (50) evaluated the feasibility of DTI in 23 patients diagnosed with schwannomas and neurofibromas using intraoperative electrical stimulation as the reference standard. The authors found that DTI tractography identified the location of nerve fibers with a 95.7% sensitivity and 66.7% specificity (maybe due to the inability of intraoperative electrical stimulation to detect sensory nerve fibers, detected by DTI). They also reported a PPV of 75% for the mapping of anatomical fiber location. The NPV was also high (93.8%); this finding suggested that tractography may be suitable to identify a "window" from which to approach the tumor resection preoperatively. Regarding the accuracy of DTI concerning tumor size, pathologi-

cal diagnosis, and tumor location, they reported improved sensitivity, PPV, and NPV in tumours arising from a distal nerve branch rather than a more proximal nerve root and for larger tumours.

In a study of Kasprian et al. (6), the feasibility of DTI in identifying peripheral nerve infiltration in cases of soft tissue tumors near peripheral nerves was assessed. In cases of malignant infiltration of peripheral nerves by adjacent soft tissue tumors, the researchers demonstrated either a change in caliber or complete disruption of the nerve on tractography images. Moreover, they were able to localize the nerve on DTI images in cases of encasement by a tumour or, in cases of peripheral nerve sheath tumors, even when the nerve was not well delineated on T2-weighted imaging. In addition, a greater tendency toward lower FA and higher ADC values for neighboring nerve segments was found in malignant STTs than in benign STTs. As in the central nervous system, this may be explained by either the higher frequency and grade of regional nerve edema associated with more aggressive tumor expansion or by true infiltration by malignant cells.

In the author's experience evaluating DTI feasibility for preoperative evaluation of peripheral nerve tumours (mainly schwannomas and neurofibromas), we noticed, in accordance with previous literature data, a reduction in FA values (mean values 0.61±0.03, range 0.43-0.88) along the course of the nerve near and around the lesion (compared to the contralateral healthy nerve) as well as a variation of the ADC values, ranging between 0.81 and 1.87x10[-3] mm2/s (mean value 1.68+0.21x10[-3] mm2/s). In cases of malignant lesions, the FA and ADC values were lower. Tractographic reconstructions were able to predict tumour location with respect to nerve fiber bundles, with good intraoperative neurosurgical findings correlation (Fig. 3, Fig. 4). Complete disruption of the nerve bundle was observed only in malignant lesions. In one case the tractography could not be performed to the non-optimal SNR/artifacts from ghosting.

Conclusions

With preoperative DTI, the relationship of the nerve tumor to the axons and nerve fascicles can be visualized and studied. Although MR DTI with tractography alone should not replace a meticulous surgical technique and careful attention to the anatomy, DTI proves to be a reliable and useful technique in helping the surgeon to plan out the safest surgical approach providing a 3D-like map of the tumor in relation to the associated nerve from which it is arising, counseling the patient on the predicted extent of

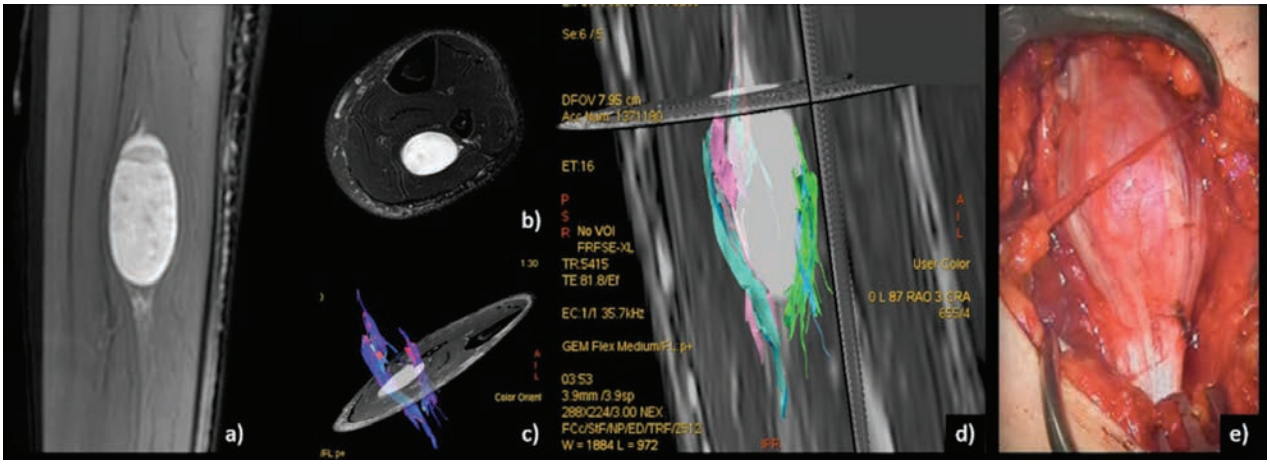

Figure 3. Post-contrast MR images (a, b) of an enhancing, fusiform lesion located at the lower third of the leg within flexor muscles. Tractography reconstructions (c, d) clearly depict in a 3D manner the relationship of the healthy nerve bundles splitted apart and arranged at the periphery of the lesion. Surgical finding (e)

Figure 4. Coronal contrast-enhanced MR slice (a) of an ovoid lesion involving the radial nerve showing inhomogeneous enhancement. 3D tractography fails to track fibers, showing a nerve fiber bundle in the lateral side of the lesion but marked nerve fiber discontinuation in the remainder, findings consistent with a neurofibroma or a degenerated schwannoma (b). Surgical finding (c)

resection and the possible compromise of nerve function.

Tractographic reconstructions provide information about neural integrity, while DTI imaging can indicate possible malignancy in neural masses evaluating diffusivity values. Thus, DTI with fiber tracking, with the functional and anatomical information provided, is a valuable tool to improve standard MR imaging techniques for the diagnosis and follow-up of nerve tumor and tumor-like conditions. Using tractography, the topographical relationship between the peripheral nerve and the tumor can be visualized unequivocally, even in the presence of marked alteration of regional anatomy where conventional sequences frequently fail to delineate clinically intact nerve structures from an encasing tumour.

The challenges of applying DTI with tractography to nerves include the relatively small size and complex course of these nerves, as well as the heterogeneity of tissues along the course of the nerves such as muscle, bone, and vasculature, which can cause an obscured background signal.

Ethical approval: This article does not contain any studies with human participants performed by any of the authors.

Conflict of interest: None to declare

References

1. Forthman CL, Blazar PE. Nerve tumors of the hand and upper extremity. Hand Clin 2004; 20: 233-42.
2. Abreu E, Aubert S, Wavreille G, Gheno R, Canella C, Cotten A. Peripheral tumor and tumor-like neurogenic lesions. Eur J Radiol 2013; 82: 38-50.
3. Stucky CC, Johnson KN, Gray RJ, et al. Malignant peripheral nerve sheath tumors (MPNST): the Mayo Clinic experience. Ann Surg Oncol 2012; 19: 878-85.
4. Ahlawat S, Chhabra A, Blakely J. Magnetic resonance neurography of peripheral nerve tumors and tumorlike conditions. Neuroimaging Clin N Am 2014; 24: 171-92.
5. Perrin RG, Guha A. Malignant peripheral nerve sheath tumors. Neurosurg Clin N Am 2004; 15: 203-16.
6. Kasprian G, Amann G, Panotopoulos J, et al. Peripheral nerve tractography in soft tissue tumors: A preliminary 3-tesla diffusion tensor magnetic resonance imaging study. Muscle Nerve 2015; 51: 338-45.
7. Di Cesare E, Patriarca L, Panebianco L, et al. Coronary computed tomography angiography in the evaluation of intermediate risk asymptomatic individuals. Radiol Med 2018; 123: 686-94.
8. Mariani S, La Marra A, Arrigoni F, et al. Dynamic measurement of patello-femoral joint alignment using weight-bearing magnetic resonance imaging (WB-MRI). Eur J Radiol 2015; 84: 2571-78.
9. Barile A, Bruno F, Arrigoni F, et al. Emergency and Trauma of the Ankle. Semi Musc Rad 2017; 21: 282-89.
10. Barile A, Bruno F, Mariani S, et al. What can be seen after rotator cuff repair: a brief review of diagnostic imaging findings. Musculoskelet Surg 2017; 101: 3-14.
11. De Filippo M, Pesce A, Barile A, et al. Imaging of postop-

erative shoulder instability. Musculoskelet Surg 2017; 101: 15-22.
12. Barile A, Arrigoni F, Bruno F, et al. Computed Tomography and MR Imaging in Rheumatoid Arthritis. Radiol Clin North Am 2017; 55: 997-1007.
13. Briganti F, Leone G, Marseglia M, Cicala D, Caranci F, Maiuri F. P64 Flow Modulation Device in the treatment of intracranial aneurysms: Initial experience and technical aspects. J Neurointerv Surg 2016; 8: 173-80.
14. Cirillo M, Caranci F, Tortora F, et al. Structural neuroimaging in dementia. J Alzheimers Dis 2012; 29: 16-19.
15. Di Cesare E, Cademartiri F, Carbone I, et al. Clinical indications for the use of cardiac MRI. by the SIRM Study Group on Cardiac Imaging. Radiol Med 2013; 118: 752-98.
16. Cappabianca S, Scuotto A, Iaselli F, et al. Computed tomography and magnetic resonance angiography in the evaluation of aberrant origin of the external carotid artery branches. Surg Radiol Anat 2012; 34: 393-99.
17. Barile A, La Marra A, Arrigoni F, et al. Anaesthetics, steroids and platelet-rich plasma (PRP) in ultrasound-guided musculoskeletal procedures. Br J Radiol 2016; 89: 20150355.
18. Zappia M, Castagna A, Barile A, Chianca V, Brunese L, Pouliart N. Imaging of the coracoglenoid ligament: a third ligament in the rotator interval of the shoulder. Skeletal Radiol 2017; 46: 1101-11.
19. Splendiani A, D'Orazio F, Patriarca L, et al. Imaging of post-operative spine in intervertebral disc pathology. Musculoskelet Surg 2017; 101: 75-84.
20. Walker EA, Fenton ME, Salesky JS, Murphey MD. Magnetic resonance imaging of benign soft tissue neoplasms in adults. Radiol Clin North Am 2011; 49: 1197-217.
21. Barile A, Regis G, Masi R, et al. Musculoskeletal tumours: Preliminary experience with perfusion MRI. Radiol Med 2007; 112: 550-61.
22. Caranci F, Briganti F, La Porta M, et al. Magnetic resonance imaging in brachial plexus injury. Musculoskelet Surg 2013; 97 Suppl 2: S181-90.
23. Reginelli A, Zappia M, Barile A, Brunese L. Strategies of imaging after orthopedic surgery. Musculoskelet Surg 2017; 101: 1.
24. Masciocchi C, Conti L, D'Orazio F, Conchiglia A, Lanni G, Barile A, Errors in Musculoskeletal MRI, in: Romano L., Pinto A. (Eds.), Errors in Radiology, Springer Milan, Milano, 2012, pp. 209-17.
25. Zappia M, Capasso R, Berritto D, et al. Anterior cruciate ligament reconstruction: MR imaging findings. Musculoskelet Surg 2017; 101: 23-35.
26. Barile A, Lanni G, Conti L, et al. Lesions of the biceps pulley as cause of anterosuperior impingement of the shoulder in the athlete: Potentials and limits of MR arthrography compared with arthroscopy. Radiol Med 2013; 118: 112-22.
27. Perrotta FM, Astorri D, Zappia M, Reginelli A, Brunese L, Lubrano E. An ultrasonographic study of enthesis in early psoriatic arthritis patients naive to traditional and biologic DMARDs treatment. Rheumatol Int 2016; 36: 1579-83.
28. Cuomo G, Zappia M, Iudici M, Abignano G, Rotondo A, Valentini G. The origin of tendon friction rubs in patients with systemic sclerosis: a sonographic explanation. Arthritis Rheum 2012; 64: 1291-93.
29. Di Pietto F, Chianca V, de Ritis R, et al. Postoperative imaging in arthroscopic hip surgery. Musculoskelet Surg 2017; 101: 43-49.
30. Perri M, Grattacaso G, Di Tunno V, et al. MRI DWI/ADC signal predicts shrinkage of lumbar disc herniation after O2-O3 discolysis. Neuroradiol J 2015; 28: 198-204.
31. Aszmann OC. Diffusion tensor tractography for the surgical management of peripheral nerve sheath tumors. Neurosurg Focus 2015; 39: 1-6.
32. Pilavaki M, Chourmouzi D, Kiziridou A, Skordalaki A, Zarampoukas T, Drevelengas A. Imaging of peripheral nerve sheath tumors with pathologic correlation: pictorial review. Eur J Radiol 2004; 52: 229-39.
33. Marampon F, Gravina G, Ju X, et al. Cyclin D1 silencing suppresses tumorigenicity, impairs DNA double strand break repair and thus radiosensitizes androgen-independent prostate cancer cells to DNA damage. Oncotarget 2016;
34. Berghmans S, Murphey RD, Wienholds E, et al. tp53 mutant zebrafish develop malignant peripheral nerve sheath tumors. Proc Natl Acad Sci U S A 2005; 102: 407-12.
35. Dalla Palma B, Guasco D, Pedrazzoni M, et al. Osteolytic lesions, cytogenetic features and bone marrow levels of cytokines and chemokines in multiple myeloma patients: Role of chemokine (C-C motif) ligand 20. Leukemia 2016; 30: 409-16.
36. Marampon F, Gravina GL, Popov VM, et al. Close correlation between MEK/ERK and Aurora-B signaling pathways in sustaining tumorigenic potential and radioresistance of gynecological cancer cell lines. Int J Oncol 2014; 44: 285-94.
37. Barile A, Quarchioni S, Bruno F, et al. Interventional radiology of the thyroid gland: Critical review and state of the art. Gland Surg 2018; 7: 132-46.
38. Barile A, Arrigoni F, Bruno F, et al. Present role and future perspectives of interventional radiology in the treatment of painful bone lesions. Future Oncol 2018; 14: 2945-55.
39. Giordano AV, Arrigoni F, Bruno F, et al. Interventional Radiology Management of a Ruptured Lumbar Artery Pseudoaneurysm after Cryoablation and Vertebroplasty of a Lumbar Metastasis. Cardiovasc Intervent Radiol 2017; 40: 776-79.
40. Arrigoni F, Bruno F, Zugaro L, et al. Role of interventional radiology in the management of musculoskeletal soft-tissue lesions. Radiol Med 2018; 1-6.
41. Cazzato RL, Arrigoni F, Emanuele Boatta, et al. Percutaneous management of bone metastases: state of the art, interventional strategies and joint position statement of the Italian College of MSK Radiology (ICoMSKR) and the Italian College of Interventional Radiology (ICIR). Radiol Med 2018; 1: 3-3.
42. Arrigoni F, Gregori LM, Zugaro L, Barile A, Masciocchi C. MRgFUS in the treatment of MSK lesions: A review based on the experience of the university of L'aquila, Italy. Transl Cancer Res 2014; 3: 442-48.

43. Ferrari F, Arrigoni F, Miccoli A, et al. Effectiveness of Magnetic Resonance-guided Focused Ultrasound Surgery (MRgFUS) in the uterine adenomyosis treatment: technical approach and MRI evaluation. Radiol Med 2016; 121: 153-61.
44. Arrigoni F, Bruno F, Zugaro L, et al. Developments in the management of bone metastases with interventional radiology. Acta Biomed 2018; 89: 166-74.
45. Arrigoni F, Barile A, Zugaro L, et al. Intra-articular benign bone lesions treated with Magnetic Resonance-guided Focused Ultrasound (MRgFUS): imaging follow-up and clinical results. Med Oncol 2017; 34: 55.
46. Tarantini G, Favaretto E, Napodano M, et al. Design and methodologies of the postconditioning during coronary angioplasty in acute myocardial infarction (POST-AMI) trial. Cardiology 2010; 116: 110-16.
47. Barile A, La Marra A, Arrigoni F, et al. Anaesthetics, steroids and platelet-rich plasma (PRP) in ultrasound-guided musculoskeletal procedures. British Journal of Radiology 2016; 89:
48. Barile A, Arrigoni F, Zugaro L, et al. Minimally invasive treatments of painful bone lesions: state of the art. Med Oncol 2017; 34: 53.
49. Gruber H, Glodny B, Bendix N, Tzankov A, Peer S. High-resolution ultrasound of peripheral neurogenic tumors. Eur Radiol 2007; 17: 2880-8.
50. Cage TA, Yuh EL, Hou SW, et al. Visualization of nerve fibers and their relationship to peripheral nerve tumors by diffusion tensor imaging. Neurosurg Focus 2015; 39: E16-E16.
51. Bruno F, Barile A, Arrigoni F, et al. Weight-bearing MRI of the knee: A review of advantages and limits. Acta Biomed 2018; 89: 78-88.
52. Michelini G, Corridore A, Torlone S, et al. Dynamic MRI in the evaluation of the spine: State of the art. Acta Biomed 2018; 89: 89-101.
53. Zhang Y, Mao Z, Wei P, et al. Preoperative Prediction of Location and Shape of Facial Nerve in Patients with Large Vestibular Schwannomas Using Diffusion Tensor Imaging–Based Fiber Tracking. World Neurosurg 2017; 99: 70-78.
54. Simon NG, Lagopoulos J, Gallagher T, Kliot M, Kiernan MC. Peripheral nerve diffusion tensor imaging is reliable and reproducible. J Magn Reson Imaging 2016; 43: 962-9.
55. Hiltunen J, Suortti T, Arvela S, Seppä M, Joensuu R, Hari R. Diffusion tensor imaging and tractography of distal peripheral nerves at 3 T. Clinical neurophysiology : official journal of the International Federation of Clinical Neurophysiology 2005;
56. Jeon T, Fung MM, Koch KM, Tan ET, Sneag DB. Peripheral nerve diffusion tensor imaging: Overview, pitfalls, and future directions. J Magn Reson Imaging 2018;
57. Skorpil M, Engstrom M, Nordell A. Diffusion-direction-dependent imaging: a novel MRI approach for peripheral nerve imaging. Magn Reson Imaging 2007; 25: 406-11.
58. Chhabra A, Thakkar RS, Andreisek G, et al. Anatomic MR imaging and functional diffusion tensor imaging of peripheral nerve tumors and tumorlike conditions. AJNR Am J Neuroradiol 2013; 34: 802-7.
59. Kronlage M, Schwehr V, Schwarz D, et al. Peripheral nerve diffusion tensor imaging (DTI): normal values and demographic determinants in a cohort of 60 healthy individuals. Eur Radiol 2018; 28: 1801-08.
60. Splendiani A, Perri M, Marsecano C, et al. Effects of serial macrocyclic-based contrast materials gadoterate meglumine and gadobutrol administrations on gadolinium-related dentate nuclei signal increases in unenhanced T1-weighted brain: a retrospective study in 158 multiple sclerosis (MS) patients. Radiol Med 2018; 123: 125-34.
61. Tedeschi E, Caranci F, Giordano F, Angelini V, Cocozza S, Brunetti A. Gadolinium retention in the body: what we know and what we can do. Radiol Med 2017; 122: 589-600.
62. Schicchi N, Valeri G, Moroncini G, et al. Myocardial perfusion defects in scleroderma detected by contrast-enhanced cardiovascular magnetic resonance. Radiol Med 2014; 119: 885-94.
63. Salvolini L, Urbinati C, Valeri G, Ferrara C, Giovagnoni A. Contrast-enhanced MR cholangiography (MRCP) with GD-EOB-DTPA in evaluating biliary complications after surgery. Radiol Med 2012; 117: 354-68.
64. Partovi S, von Tengg-Kobligk H, Bhojwani N, Karmonik C, Maurer M, Robbin MR. Advanced Noncontrast MR Imaging in Musculoskeletal Radiology. Radiol Clin North Am 2015; 53: 549-67.
65. Rangavajla G, Mokarram N, Masoodzadehgan N, Pai SB, Bellamkonda RV. Noninvasive imaging of peripheral nerves. Cells Tissues Organs 2014; 200: 69-77.
66. Chhabra A, Madhuranthakam AJ, Andreisek G. Magnetic resonance neurography: current perspectives and literature review. Eur Radiol 2018; 28: 698-707.
67. Cauley KA, Filippi CG. Diffusion-tensor imaging of small nerve bundles: Cranial nerves, peripheral nerves, distal spinal cord, and lumbar nerve roots- Clinical applications. Am J Roentgenol 2013; 201: 326-35.
68. Jambawalikar S, Baum J, Button T, Li H, Geronimo V, Gould ES. Diffusion tensor imaging of peripheral nerves. Skeletal Radiol 2010; 39: 1073-79.
69. Eppenberger P, Andreisek G, Chhabra A. Magnetic resonance neurography. Diffusion tensor imaging and future directions. Neuroimaging Clin N Am 2014; 24: 245-56.
70. Khalil C, Budzik JF, Kermarrec E, Balbi V, Le Thuc V, Cotten A. Tractography of peripheral nerves and skeletal muscles. Eur J Radiol 2010; 76: 391-97.
71. Valeri G, Mazza FA, Maggi S, et al. Open source software in a practical approach for post processing of radiologic images. Radiol Med 2015; 120: 309-23.
72. Vargas MI, Viallon M, Nguyen D, Delavelle J, Becker M. Diffusion tensor imaging (DTI) and tractography of the brachial plexus: Feasibility and initial experience in neoplastic conditions. Neuroradiology 2010.
73. De Filippo M, Onniboni M, Rusca M, et al. (2008). Advantages of multidetector row CT with multiplanar reformation in guiding percutaneous lung biopsies. RAD. MED, vol.

113, p. 945-953, ISSN: 0033-8362, doi: 10.1007/s11547-008-0325-y
74. Bertolini L, Vaglio A, Bignardi L, et al (2011). Subclinical interstitial lung abnormalities in stable renal allograft recipients in the era of modern immunosuppression. Transplantation Proceedings, vol. 43, p. 2617-2623, ISSN: 0041-1345, doi: 10.1016/j.transproceed.2011.06.033.
75. Palma BD, Guasco D, Pedrazzoni M, et al. Osteolytic lesions, cytogenetic features and bone marrow levels of cytokines and chemokines in multiple myeloma patients: Role of chemokine (C-C motif) ligand20. Leukemia. 2016 Feb;30(2):409-16. doi: 10.1038/leu.2015.259. Epub 2015 Sep 30.
76. Bozzetti C, Nizzoli R, Tiseo M, et al. ALK and ROS1 rearrangements tested by fluorescence in situ hybridization in cytological smears from advanced non-small cell lung cancer patients. Diagnostic Cytopathology, vol. 43, p. 941-946, ISSN: 8755-1039, doi: 10.1002/dc.23318.
77. De Filippo M, Gira F, Corradi D, Sverzellati N, Zompatori M, Rossi C. (2011). Benefits of 3D technique in guiding percutaneous retroperitoneal biopsies. RAD. MED, vol. 116(3), p. 407-416, ISSN: 0033-8362, doi: 10.1007/s11547-010-0604-2.
78. Barile A, Bruno F, Mariani S, et al. What can be seen after rotator cuff repair: a brief review of diagnostic imaging findings. Musculoskelet Surg. 2017 Mar;101(Suppl 1):3-14. doi: 10.1007/s12306-017-0455-2. Epub 2017 Feb 13. Review.

Received: 26 March 2019
Accepted: 4 April 2019
Correspondence:
Federico Bruno, M.D.
Department of Biotechnology and Applied Clinical Sciences
University of L'Aquila,
Vetoio Street 1 - 67100 L'Aquila, Italy
Tel. +390862368512
E-mail: federico.bruno.1988@gmail.com